Calculation of *z*-Coordinates and Orientational Restraints Using a Metal Binding Tag[†]

Vadim Gaponenko,[‡] Alex Dvoretsky,[‡] Charles Walsby,[§] Brian M. Hoffman,[§] and Paul R. Rosevear*,[‡]

Department of Molecular Genetics, Biochemistry, and Microbiology, University of Cincinnati, College of Medicine, Cincinnati, Ohio 45267, and Department of Chemistry, Northwestern University, Evanston, Illinois 60208

Received June 16, 2000; Revised Manuscript Received September 27, 2000

ABSTRACT: We introduce a new simple methodology allowing the measurement of ^{1}H-^{15}N residual dipolar couplings, dipolar shifts, and unpaired electron−amide proton distances. This method utilizes a zinc finger tag fused at either the N- or the C-terminus of a protein. We have demonstrated this fusion strategy by incorporating the zinc finger of the retroviral gag protein onto the C-terminus of barnase, a ribonuclease produced by *Bacillus amiloliquifaciance.* We show that this tag can be substituted with cobalt and manganese. Binding of cobalt to the gag zinc finger−barnase fusion protein introduced sufficient anisotropic paramagnetic susceptibility for orientation of the molecule in the magnetic field. Partial alignment permitted measurement of $^1J_{HN}$ scalar couplings along with dipolar couplings. Replacement of bound cobalt with diamagnetic zinc removes the paramagnetic-induced orientation of barnase, permitting the measurement of only $^1J_{HN}$ scalar couplings. Dipolar couplings, ranging from −0.9 to 0.6 Hz, were easily measured from the difference in splitting frequencies in the presence of cobalt and zinc. The observed paramagnetic anisotropy induced by cobalt binding to the metal binding tag also permitted measurement of dipolar shifts. Substitution of manganese into the metal binding tag permitted the measurement of unpaired electron−amide proton distances using paramagnetic relaxation enhancement methodology. The availability of both amide proton dipolar shifts and unpaired electron to amide proton distances permitted the direct calculation of *z*-coordinates for individual amide protons. This approach is robust and will prove powerful for global fold determination of proteins identified in genome initiatives.

Residual dipolar couplings and dipolar shifts have been shown to provide important long-range orientational restraints for structure determination (*1*, *2*). Dipolar contributions to scalar couplings can be observed when the molecule has sufficient alignment in the magnetic field. Dipolar couplings have previously been measured in a number of paramagnetic proteins, such as cyanometmyoglobin (*3*). In addition, binding of a paramagnetic metal either to the ADR1 zinc finger or to a His tag fused to either the N- or the C-terminus of a protein has been used to achieve partial alignment of the target protein in a magnetic field (*4*, *5*). Dipolar shifts occur in magnetically anisotropic paramagnetic systems when there is a sizable dipolar interaction between the electronic magnetic moment and the nuclear spin magnetic dipole. The usefulness of dipolar shifts in structure refinement of paramagnetic proteins has been well documented (*6*−*10*).

Alignment of nonmetalloproteins in the external field has been achieved by the use of liquid-crystalline media. For example, dihexanoylphosphatidylcholine and dimyristoylphosphatidylcholine mixtures at room temperatures form discoid particles that orient in the magnetic field. At low concentrations, the spacing between individual bicelles allows protein molecules to align with respect to the external magnetic field, but still diffuse in the aqueous solution. This permits precise measurement of residual dipolar couplings while preserving the quality of NMR[1] spectra (*2*). This approach can be used to achieve high degrees of alignment. However, maintenance of the bicelles can be difficult under the conditions necessary for stabilizing the structure and/or function of proteins. More recently, phage particles have been utilized to obtain partial alignment of proteins and nucleic acids in the external magnetic field (*11*−*13*). Large dipolar couplings of 45−50 Hz in magnitude can be routinely obtained for ^{1}H-^{15}N vectors (*2*). A potential drawback of this methodology is the possibility of strong electrostatic interactions between the biomolecule and the phage particles which can result in increased transverse relaxation rates.

Here we demonstrate a simple technique for affinity purification and partial alignment of proteins in solution. This method utilizes a cobalt binding zinc finger tag fused at either

[†] This work is supported by Grant AR 44324 (P.R.R.) from the National Institutes of Health, by Grant MCB-9904018 from the National Science Foundation, and by USDA Grant 97-37305-4879 (B.M.H.).

* To whom correspondence should be addressed at the Department of Molecular Genetics, Biochemistry, and Microbiology, University of Cincinnati, College of Medicine, 231 Bethesda Ave., Cincinnati, OH 45267. Phone: 513-558-3370; fax: 513-558-8474; email: rosevear@proto.med.uc.edu.

[‡] University of Cincinnati.

[§] Northwestern University.

[1] Abbreviations: NMR, nuclear magnetic resonance; EPR, electron paramagnetic resonance; HSQC, heteronuclear single quantum coherence spectroscopy; *R*, correlation coefficient; ZFS, zero-field splitting; C-ZFbarnase, barnase(H102A) containing the sequence DQCAYCK-EKGHWAKECPK cloned to a linker sequence (SG) at the C-terminus of the barnase (H102A) gene; a/b TROSY, spin-selective transverse relaxation optimized spectroscopy; $1/T_1$, ^{1}H longitudinal relaxation rate; $1/T_{1p}$, paramagnetic contribution to ^{1}H longitudinal relaxation rate.

10.1021/bi001381w CCC: $19.00
Published on Web 11/15/2000

the N- or the C-terminus of a protein. We have utilized this fusion strategy by incorporating the zinc finger of the retroviral gag protein onto the C-terminus of barnase, a ribonuclease produced by *Bacillus amiloliquifaciance*. The structure of barnase is well-known (*14*). Binding of cobalt to the gag zinc finger−barnase fusion protein (C-ZFbarnase) introduced sufficient anisotropic paramagnetic susceptibility for orientation of the molecule in the magnetic field, permitting measurement of $^1J_{HN}$ scalar couplings along with dipolar couplings. The relaxation time for the cobalt electron spin is fast, preserving the high resolution of NMR spectra at high field. Replacement of bound cobalt with diamagnetic zinc removes the paramagnetically induced orientation of barnase, and only scalar couplings are observed. Residual dipolar couplings can be easily measured from the difference in splitting frequencies under these two conditions. In a similar manner, the paramagnetic anisotropy, induced by the cobalt binding zinc finger, was used to measure dipolar shifts. Unpaired electron−^1H_N distances were also measured using paramagnetic relaxation enhancement methodology on the Mn^{2+}-substituted gag-tagged protein (*15*). The combination of both ^1H_N dipolar shifts and unpaired electron−^1H_N distances permitted direct calculation of the *z*-coordinates for amide protons in gag-tagged barnase. The experimentally determined *z*-coordinates can be utilized in both structure determination and refinement.

MATERIALS AND METHODS

Fusion Construction, Expression, and Purification. The zinc finger sequence coding for Asp-Gln-Cys-Ala-Tyr-Cys-Lys-Glu-Lys-Gly-His-Trp-Ala-Lys-Glu-Cys-Pro-Lys was cloned into the *Bam*HI and *Not*I sites of the pET23d+ expression vector to allow convenient tagging of barnase or any other protein. To clone the gag tag into pET23d+, two complimentary oligos were synthesized: 5′ GAT CCG ACC AGT GCG CTT ACT GCA AAG AAA AAG GTC ACT GGG CTA AAG AAT GCC CGA AAT GCC CGA AAT AGT AAG C 3′ and 5′ GGC CGC TTA CTA TTT CGG GCA TTC TTT AGC CCA GTG ACC TTT TTC TTT GCA GTA AGC GCA CTG GCT G 3′.

The 100 μM solutions of the oligos were mixed in equimolar concentrations. The mixture was incubated at 94 °C for 5 min. Then five 5 °C cooling steps with a duration of 5 min were used to bring the temperature down from 85 °C to 60 °C. After annealing, a ligation reaction into the *Bam*HI and *Not*I restriction sites of the pET23d+ expression vector was performed. The cDNA sequence of mutant barnase, H102A, was cloned into the *Nco*I and *Bam*HI restriction sites. The H102A mutation in the active site of barnase was used to improve overexpression, since the wild-type protein is known to be toxic to *E. coli* cells (*16*). It has previously been shown that mutation of His102 in barnase does not affect the stability or the structure of the protein (*15*, *17*). The fusion protein was expressed in BL21(DE3) cells and purified as described previously (*15*). About 60% of the protein was purified as a dimer induced by formation of disulfide bridges in the metal binding tag. Dimerization was found to prevent binding of adventitious metals to the metal binding tag. After reduction with 50 mM DDT, the protein was dialyzed against buffer containing 10% ^2H_2O, 50 mM NaCl, and 20 mM HEPES, pH 7.4. Alternatively, one-step purification on a nickel column (Novagen) was used to obtain purified tagged protein. The purification procedure was performed in the following manner. To prevent dimer formation, 10 mM β-mercaptoethanol was added to the protein containing supernatant. To prevent reaction of the reducing agent with Ni^{2+} ions, the protein solution was passed over a P4 column equilibrated in the following buffer: 5 mM imidazole, 500 mM NaCl, and 20 mM Tris-HCl, pH 8. The pH was adjusted to 8. The charged Novagene resin (5 mL of resin slurry per 1 L of culture) was immediately added to the reduced protein solution. The resin was incubated with the protein for 1 h at 4 °C with slow stirring. The resin was allowed to settle, and a small column was packed. The column was washed with 10 volumes of buffer containing 5 mM imidazole, 500 mM NaCl, and 20 mM Tris-HCl, pH 8. Subsequently, 6 volumes of the wash buffer (60 mM imidazole, 500 mM NaCl, and 20 mM Tris-HCl, pH 8) were used to remove nonspecifically bound proteins. The protein was eluted with 6 volumes of the elution buffer (100 mM EDTA, 500 mM NaCl, and 20 mM Tris-HCl, pH 8). The protein purity was judged by SDS−PAGE gel electrophoresis and staining with Coomassie Brilliant Blue. The purified fusion protein containing the gag-tag located at the C-terminus of barnase(H102A) is abbreviated as C-ZFbarnase.[1]

Metal Binding. Protein concentrations were determined by Bradford (BioRad) and by the UV absorbance at 280 nm using a molar extinction coefficient of 2.1 (0.1% absolute, g/L) (*18*). Preparation of 0.7 mM Co^{2+}-substituted C-ZFbarnase by 0.1 mM step titration with $CoCl_2$ was monitored using visible spectroscopy as previously described (*19*). Manganese-substituted gag-tagged barnase was prepared by titration of 0.1 molar equiv of $MnCl_2$ into 0.5 mM metal-free (dialyzed against 50 mM EDTA with subsequent removal of the chelating agent) protein solution. Titration was monitored by NMR using line width analysis. The line widths were obtained using the Lorentzian line shape fitting routine incorporated into the Felix 2000 software (MSI). Upon saturation of the metal binding tag with Mn^{2+} at a protein to metal molar ratio of 1:0.75, a slight linear increase in the ^1H_N line widths was observed. This could be explained by paramagnetic relaxation enhancement by free or weakly bound Mn^{2+}. At this point, Mn^{2+}-loaded C-ZFbarnase was dialyzed against Chelex-100 (Sigma) treated NMR buffer to remove any excess Mn^{2+}.

EPR and NMR Spectroscopy. The symmetry of the magnetic susceptibility created by Co^{2+}-bound C-ZFbarnase was deduced from a 35 GHz Q-band EPR spectrum at 2 K on a modified Varian E-110 spectrometer equipped with a helium immersion dewar (*20*). The **g** tensor parameters were determined using the equations:

$$\Delta\chi_{axial} = \chi_{||} - \chi_{\perp} \quad (1)$$

$$\bar{\chi}_{kk} = \frac{\mu_0 \mu_B{}^2 S(S+1)}{3kT} \bar{g}_{kk}{}^2 \quad (2)$$

where μ_B is the Bohr magneton, μ_0 is the vacuum permeability, k is the Boltzmann constant, T is the absolute temperature, and $\bar{g}_{kk}$ is a mean principal value of the **g** tensor.

NMR experiments were performed on Varian Inova 500, 600, and 800 MHz spectrometers at 30 °C. Resonance assignments for ^1H-^{15}N correlations in [^{15}N]C-ZFbarnase

were confirmed by a three-dimensional NOESY−HSQC experiment with a 70 ms mixing time and compared with those reported for wild-type barnase (*16*) and barnase-(H102A) (*15*). *T*1 inversion recovery ^{1}H-^{15}N HSQC spectra were collected with 200, 400, 600, 800, 1000, 1200, 1400, 1600, 1800, and 2000 ms delay times on both the Zn^{2+}- and Mn^{2+}-loaded [^{15}N]C-ZFbarnase, as described previously (*15*). For some H_N protons, additional data points at 10 and 3000 ms were obtained to improve *T*1 data fits. Double points were used to estimate the error in *T*1 measurements. Spectra were processed using Felix software (MSI, San Diego, CA) with resolution enhancement (90°) shifted sine-bell squared function in both dimensions. Peak intensities were measured for both the Zn^{2+}- and Mn^{2+}-loaded [^{15}N]C-ZFbarnase proteins. The values were fitted to the following equation (*21*):

$$I(\tau) = I_D[1 - B(1 - \exp^{(-\kappa/T1)}) \times \exp^{(-\tau/T1)}] \quad (3)$$

where κ is the sum of acquisition and preparation times, *B* is an adjustment parameter for incomplete magnetization inversion, τ is the recovery delay, and *T*1 is the longitudinal relaxation time. Paramagnetic effects on amide proton relaxation rates were calculated using

$$\frac{1}{T1_p} = \frac{1}{T1_{Mn^{2+}}} - \frac{1}{T1_{dia}} \quad (4)$$

where $T1_p$ is the paramagnetic effect on the amide proton longitudinal relaxation times, $T1_{Mn^{2+}}$ is the longitudinal relaxation time of the manganese-bound protein, and $T1_{dia}$ is the amide proton longitudinal relaxation time of C-ZFbarnase loaded with Zn^{2+} (*15*). Correlation times, τ_c, for the amide protons were estimated from the frequency dependence of the paramagnetic effects at 600 and 500 MHz using the following equation (*22*):

$$\tau_c^{\,2} = \frac{T1_{p600} - T1_{p500}}{T1_{p600}\omega_{500}^{\,2} - T1_{p500}\omega_{600}^{\,2}} \quad (5)$$

Frequency independence of τ_c was assumed. Estimates in the distance, *r*, are relatively insensitive to small errors in τ_c, since *r* depends on the sixth-root of the correlation time (*23*). Distances were calculated using the Solomon−Bloembergen equation (*24*):

$$r^6 = \frac{2}{15}\frac{S(S+1)g^2\gamma_H^2\beta^2}{T1_p} \times \frac{3\tau_c}{1 + \omega_H^2\tau_c^{\,2}} \quad (6)$$

where ω_H is the^{1}H Larmor precession frequency. The total number of experimentally determined distances was 43. The following data points could not be obtained due to spectral overlap: 3, 14, 24, 35, 39, 49, 60, 63, 73, 74, 77, 78, 82, 84, 87, 99, 101, and 104. Cross-peaks for residues 4, 11, 12, 15−19, 22, 37, 38, 45, 55, 57, 58, 66, 67, 85, 89, 91, and 93 were not observed due to H_N exchange at high pH. The C-terminal residues 108, 109, and 110 were excluded from the analysis because of conformational instability at the tag attachment site. For residues 25, 26, 41, 42, 50, 51, 68, 69, 70, 76, 83, 86, 92, 95, 96, 97, 102, and 103, assignments could not be confirmed, since sequential NOEs were not observed. Residues 21 and 47 are prolines. Accurate relaxation measurements could not be obtained for residue 75.

The location of the paramagnetic center was determined by minimizing the following function with respect to the coordinates of the paramagnetic center:

$$\Delta_r = \sum(r - \hat{r})^2 \quad (7)$$

where *r* is the experimentally determined $Mn^{2+}-H_N$ distance and $\hat{r}$ is the calculated $Mn^{2+}-H_N$ distance.

Dipolar couplings were collected using a generalized a/b TROSY experiment. The experiment was performed on Zn^{2+}-bound (not oriented) and on Co^{2+}-bound (partially oriented) proteins. Dipolar couplings were obtained from the differences in couplings observed in partially oriented and nonoriented samples. Dipolar couplings were calculated using the following equation:

$$\hat{D}_{HN} = \frac{\gamma_H\gamma_N h}{8\pi^3 r^3}\left[\frac{B^2}{15kT}\right]\frac{\chi_{ax}}{2}(1 - 3\cos^2\theta) \quad (8)$$

where $\hat{D}_{HN}$ is the calculated dipolar coupling, χ_{ax} is the axial component of the paramagnetic susceptibility, γ_N is the ^{15}N gyromagnetic ratio, γ_H is the proton gyromagnetic ratio, *h* is the Planck constant, *B* is the magnetic field strength, *k* is the Boltzmann constant, *r* is the amide proton−amide nitrogen distance, *T* is the absolute temperature, and θ is the angle between the *z*-axis of the susceptibility tensor and the amide proton−amide nitrogen vector. Dipolar couplings were used in an alignment tensor fitting procedure based on the known structure of barnase (*14*) in order to determine the three Euler angles, α, β, and γ, that define the relationship between the paramagnetic and the crystal structure reference frames. This was accomplished by minimizing the following target function with the Euler angles α, β, and γ and anisotropy components $\Delta\chi_{ax}$ and $\Delta\chi_{rh}$:

$$\Delta_{HN} = \sum(D_{HN} - \hat{D}_{HN})^2 \quad (9)$$

where D_{HN} is the experimentally measured dipolar coupling and $\hat{D}_{HN}$ is the calculated dipolar coupling.

Dipolar shifts were measured as H_N chemical shift differences between Co^{2+}-loaded and Zn^{2+}-loaded [^{15}N]C-ZFbarnase from high-resolution 600 MHz ^{1}H-^{15}N HSQC spectra using ^{1}H and ^{15}N spectral widths of 12 and 3.2 kHz, respectively, and 1024 increments in the indirect dimension. Angular information was obtained using the following equation:

$$\Delta\delta = \frac{\chi_{ax}}{3r^3}(1 - 3\cos^2\theta) \quad (10)$$

where $\Delta\delta$ is the observed dipolar shift, χ_{ax} is the axial component of the paramagnetic susceptibility, *r* is the unpaired electron−nucleus distance, and θ is the angle between the *z*-axis of the susceptibility tensor and unpaired electron−amide proton vector.

The observed dipolar shifts were used in a least-squares fitting procedure to define the position of the paramagnetic susceptibility tensor relative to the crystal structure of barnase (*14*). The orientation of the paramagnetic susceptibility tensor

was assumed to be equal to the orientation of the alignment reference frame determined from the analysis of the dipolar couplings. The principal component was initially set to -1.6510^{-31} m^3, the value obtained by EPR. The coordinates for the paramagnetic center were those determined from the minimization of the experimentally determined distances. The Euler angles, α, β and γ, which define the relationship between the reference frame of the paramagnetic susceptibility tensor and the physical reference frame of the structure, were obtained from the minimization of the dipolar couplings.

The following target function was minimized with respect to the anisotropy components $\Delta\chi_{ax}$ and $\Delta\chi_{rh}$:

$$\Delta_{dip} = \sum(\Delta\delta_{dip} - \Delta\hat{\delta}_{dip})^2 \quad (11)$$

where $\Delta\delta_{dip}$ and $\Delta\hat{\delta}_{dip}$ are the observed and calculated dipolar shift values, respectively.

The Generalized Reduced Gradient nonlinear optimization method from the Solver Dynamic Link Library, Version 3.5 (Frontline Systems Inc.), was used for the minimization procedure. A tolerance of 5% and a convergence value of 0.001 were utilized. The described minimization protocol allowed determination of the absolute orientation of the paramagnetic susceptibility tensor for Co^{2+} bound to C-ZFbarnase. All residues with known H_N and ^{15}N dipolar shifts were utilized in the tensor fitting procedure.

Calculation of z-Coordinates. Projections of the metal$-^1H_N$ vectors onto the principal axis of the paramagnetic susceptibility tensor were calculated using the following equation:

$$z = r\cos\theta \quad (12)$$

where r is the metal$-^1H_N$ distance determined by means of paramagnetic relaxation enhancement methodology and θ is the angle between the metal$-^1H_N$ vector and the principal axis of the paramagnetic susceptibility tensor.

RESULTS

Construction of C-ZFbarnase Fusion Protein. To evaluate the strategy of using metal binding tags to induce anisotropy and partial alignment of a target protein, a zinc finger sequence coding for the retroviral gag zinc finger was fused to the C-terminus of barnase(H102A).

The zinc finger amino acid sequence used in this research is essentially that published by Green et al. derived from the nucleic acid binding protein from Rauscher murine leukemia virus (*25*). The reason for choosing this tag is its high affinity for both zinc (diamagnetic metal) and cobalt (paramagnetic metal). The dissociation constant for cobalt was reported to be 1 μM at pH 7.0 (*25*). Zinc readily displaces cobalt from the zinc finger peptide. Also, it takes a large excess of a good chelating agent, such as EDTA, to remove the bound metal from the zinc finger (*25*). Since, manganese can substitute for either cobalt or zinc, we could reasonably expect that a Mn^{2+}-substituted form of this fusion protein could also be obtained (*26, 27*). Paramagnetic manganese, when bound to protein molecules, commonly induces a spherically symmetrical magnetic field. This property makes it a good candidate for use as a probe of distance-dependent changes in proton longitudinal relaxation rates. Resonance assignments for ^1H-^{15}N correlations in zinc-loaded C-ZFbarnase were confirmed by a three-dimensional NOESY−HSQC experiment and compared with those reported for wild-type barnase (*28*) as previously described (*15*).

Absolute values for H_N chemical shift differences between [^{15}N]barnase and [^{15}N]C-ZFbarnase were obtained. Differences in chemical shifts reflect differences in environments sensed by the nuclei that arise primarily because of structural perturbations. The fact that no significant amide ^1H chemical shift differences were observed between wild-type barnase and C-ZFbarnase demonstrated that neither the His to Ala mutation nor the C-terminal gag tag perturbed the barnase structure.

Calculations of H_N z-Coordinates from $Mn^{2+}-H_N$ Distances and Co^{2+}-Induced Dipolar Shifts. Manganese binding to the apo gag-tag fusion protein was monitored using ^{15}N-edited HSQC experiments. Titration of 0.5 mM protein solution with $MnCl_2$ was performed in 0.1 mM steps. Complete saturation of the Mn^{2+} binding site was achieved at a protein to metal molar ratio of 1:0.75 as judged by ^1H_N line-broadening. Excess Mn^{2+} resulted in a linear increase in line widths due to outer sphere relaxation effects and was removed by washing the C-ZFbarnase sample with NMR buffer in an Amicon concentrator. Line width analysis of $^{15}N-^1H$ cross-peaks as a function of [Mn^{2+}] yielded an approximate binding constant of 10 μM.

Longitudinal relaxation rates for H_N protons in Mn^{2+}- and Zn^{2+}-bound C-ZFbarnase were collected using inversion recovery experiments at 500 and 600 MHz as previously described (*15*). To ensure that there was no detectable contribution to ^1H_N relaxation rates from nonspecifically bound or free Mn^{2+}, [^{15}N]barnase(H102A) was treated with $MnCl_2$ in the same manner as the fusion protein, and H_N relaxation rates were measured. These relaxation rates were found to be in agreement with those collected on the Zn^{2+}-bound fusion protein, suggesting no significant paramagnetic contribution of nonspecifically bound Mn^{2+}.

Analysis of paramagnetic relaxation enhancements in terms of distance measurements was based on several assumptions. First, the effects of zero-field splitting at high fields were considered to be negligible. Second, to the first approximation, the electronic relaxation time was considered to be field independent. This assumption is based on several observations reported in the literature showing that the error contribution to τ_C calculations is generally larger than contributions from the field dependence of the Mn^{2+} relaxation time (*29, 30*). A correlation time, τ_C, of 1.2 ns was estimated based on the field dependence of the paramagnetic effects on longitudinal relaxation rates at ^1H precession frequencies of 500 and 600 MHz. The paramagnetic enhancement on the longitudinal relaxation rate was determined from the difference in relaxation rates in Mn^{2+}-bound and Zn^{2+}-bound C-ZFbarnase. A total of 43 unpaired electron$-H_N$ distances were calculated using the Solomon−Bloembergen equation as described previously using the τ_C value estimated as described above and the measured paramagnetic effects on the longitudinal relaxation rates, $1/T_{1p}$ (*15*).

Unexpectedly, a range of Mn^{2+} to H_N distances between 30 and 60 Å was calculated (Figure 1). However, the longer distances were found to correlate with the small magnitude

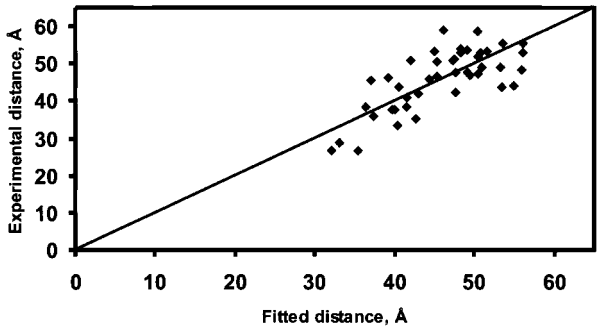

FIGURE 1: Scatter plot showing the correlation between experimentally determined electron−H_N distances in Mn^{2+}-labeled C-ZFbarnase and distances between the fitted position of the unpaired electron and H_N nuclei in the crystal structure of barnase (*14*). Experiments were performed on a 500 MHz spectrometer at 30 °C. The protein concentration was 0.5 mM. NMR buffer contained 20 mM HEPES (pH 7.4), 50 mM NaCl, and 10% D_2O. The position of the paramagnetic center relative to the barnase crystal structure was determined as described under Materials and Methods.

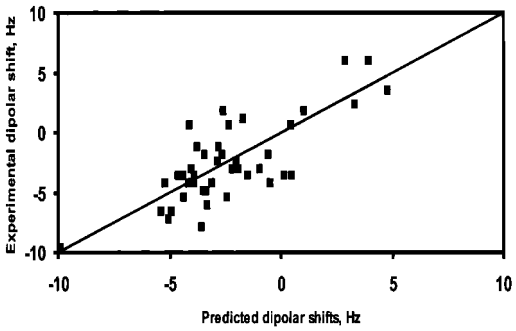

FIGURE 2: Scatter plot showing the correlation between observed ^1H_N dipolar shifts and those predicted based on the crystal structure of barnase. The correlation coefficient is 0.58. The experimental values were measured in a ^1H-^{15}N correlation HSQC spectrum at 600 MHz. The protein concentration was 0.7 mM. NMR buffer composition was 20 mM HEPES (pH 7.4), 50 mM NaCl, and 10% D_2O. A least-squares fitting procedure was used to obtain the predicted values of dipolar shifts based on the barnase crystal structure.

of measured dipolar shifts in Co^{2+}-loaded C-ZFbarnase (see below). Based on the structure, the distance between the N-terminus of the zinc finger tag and the metal ion is approximately 14 Å. Introduction of the two extra residues due to the cloning site accounts for an additional 7−10 Å. In addition, the closest amide proton resonances in the C-terminus of barnase were not observed due to exchange broadening. Thus, the range of estimated distances is consistent with the known structural restraints and measured dipolar shifts.

The experimentally determined distances were used to fit the position of the paramagnetic probe with respect to the structure of barnase (*14*) using a least-squares fitting procedure. The correlation between fitted Mn^{2+} to H_N and experimentally determined distances was reasonably good with the correlation coefficient of 0.74 and an average standard deviation of 4.5 Å (Figure 1). The somewhat large deviation from the linear fit observed for some distances may be explained by the mobility of the Mn^{2+}-bound zinc finger tag. To further investigate this possibility, ^{15}N transverse relaxation rates were collected for Zn^{2+}-bound C-ZFbarnase and barnase(H102A). The most significant difference was observed for C-terminal barnase residues 106−110. In barnase(H102A), the R_2 values for those residues are decreased, indicating flexibility commonly observed for terminal residues in proteins. In the tagged protein, the R_2 values for residues 106, 107, and 108 show larger average R_2 values, indicating conformational exchange. Correlations for residues 109 and 110 are broadened beyond detection, further supporting the argument about conformational exchange at the attachment site for the zinc finger tag.

Titration of 0.7 mM apo [^{15}N]C-ZFbarnase solution with $CoCl_2$ in 0.1 mM steps was monitored using UV−visible spectroscopy. A chromophore with absorbances at 350, 643, and 685 nm was formed (data not shown). This result is consistent with tetraheral binding of cobalt to the zinc finger tag. The saturation point determined the proper cobalt-to-protein ratio to form a 1:1 complex.

The symmetry of the magnetic susceptibility created by cobalt was deduced from a Q-band EPR spectrum at 2 K. The $S = 3/2$ spin manifold of Co(II) is split into two doublets by the zero-field splitting (ZFS; axial and rhombic parameters, D and E, rhombicity, $\lambda = |E/D|$) (*31*). At ambient temperature, the susceptibilities are expected to be determined by the averages of the g values for the two doublets: $\bar{g}_x \approx g_e$, $\bar{g}_y \approx g_e(1 + 3\lambda)(1 + 3\lambda^2)^{1/2}$, $\bar{g}_z \approx 2g_e/(1 + 3\lambda^2)^{1/2}$. The EPR spectrum suggests that the ZFS interaction approaches the limit of complete rhombicity ($\lambda = 1/3$), in which case the average **g** tensor becomes axial, with: $\bar{g}_\perp \approx g_e \times \sqrt{3} \sim 3.5$; $\bar{g}_{||} \approx g_e \sim 2$. The magnetic susceptibility anisotropy in this case is related to the average g values through eqs 1 and 2. Using these equations, the value of $\Delta\chi_{axial}$ is calculated to be -1.6×10^{-31} m^3.

Binding of cobalt was found to induce measurable differences in H_N and $^{15}N_H$ chemical shifts. Dipolar shifts for H_N were measured using ^{15}N-edited HSQC experiments on Co^{2+}- and Zn^{2+}-bound C-ZFbarnase. Measured dipolar shifts were small, ranging from 0 to ±0.05 ppm. The small size of the observed dipolar shifts is consistent with large unpaired electron−nucleus distances. Importantly, the magnitude of these shifts did not impede resonance assignments in the fusion protein.

To demonstrate the correlation between protein structure and measured dipolar shifts, dipolar shifts were fitted to the known structure of barnase, and the fitted values were then compared with those experimentally observed (Figure 2). Although the correlation coefficient was 0.58, the fitted value for paramagnetic susceptibility of -1.3×10^{-31} m^3 was in agreement with the value obtained by EPR. The low correlation coefficient was largely the result of errors in the measurement of the small dipolar shifts.

Using the magnetic susceptibility parameters obtained by EPR and unpaired electron−H_N distances, angles between the z-axis of the susceptibility tensor derived from dipolar shifts and unpaired electron−H_N vectors were calculated from eq 10. These angles and experimentally determined electron−H_N distances were used to calculate projections of positions for H_N nuclei in barnase onto the z-axis of the paramagnetic susceptibility tensor (Figure 3). Crystal structure coordinates for barnase (*14*) were translated to the paramagnetic frame of reference for comparison with the experimentally determined z-coordinates. A reasonably good linear correlation was observed with an R value of 0.72 (Figure 3A). To evaluate the major source of error, experimentally determined distances were used to fit the position

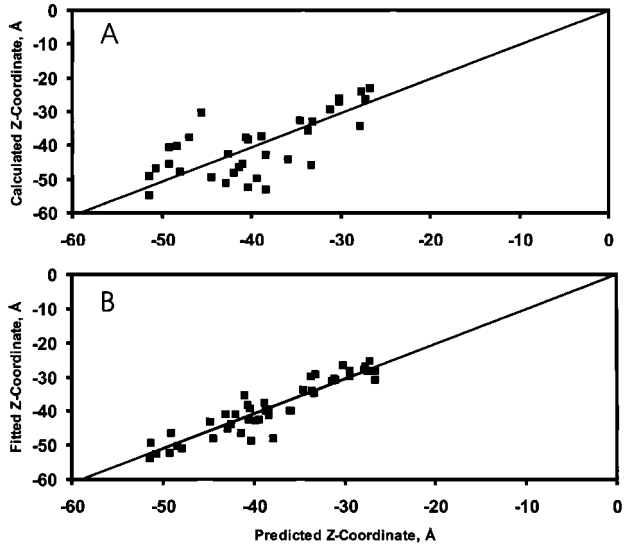

FIGURE 3: Scatter plot showing experimentally determined projections of positions for H_N nuclei in barnase onto the *z*-axis of the paramagnetic susceptibility tensor versus *z*-coordinates for H_N nuclei in the crystal structure of barnase (9). The PDB coordinates were translated to the paramagnetic frame of reference to compare the experimentally determined and calculated *z*-coordinates. (A) The experimental *z*-coordinates were calculated from experimentally determined $Mn^{2+}-H_N$ distances and angles between electron$-H_N$ vectors and the *z*-axis of the paramagnetic susceptibility tensor derived from dipolar shifts. (B) The experimentally determined $Mn^{2+}-H_N$ distances were used to fit the position of the paramagnetic center with respect to the crystal structure of barnase (9). The electron$-H_N$ distances were then calculated using the position of the paramagnetic center and the crystal structure of barnase. These distances and the angles between electron$-H_N$ vectors and the *z*-axis of the paramagnetic susceptibility tensor derived from dipolar shifts were used to calculate *z*-coordinates.

of the paramagnetic center with respect to the known structure of barnase. The electron$-H_N$ distances were then mathematically calculated using the position of the paramagnetic probe and the crystal structure of barnase. These distances and the angles between electron$-H_N$ vectors and the *z*-axis of the paramagnetic susceptibility tensor were used to calculate *z*-coordinates. The correlation coefficient between these *z*-projections and coordinates for barnase was 0.86 (Figure 3B). This improvement in the linear fit indicates the major contribution to errors in the *z*-coordinates derives from errors in measurements of the long Mn^{2+} to H_N distances. The two positions for the paramagnetic center derived from the dipolar shift fitting and distance fitting to the crystal structure of barnase (*14*) were only 2.5 Å apart as depicted in Figure 4.

Measurement of Residual Dipolar Couplings for H−N Bond Vectors in Co^{2+}-Labeled [^{15}N]C-ZFbarnase. Dipolar couplings were collected using a generalized a/b TROSY experiment (*32*). The experiment was performed on zinc-bound (not oriented) and on cobalt-bound (partially oriented) proteins. Measured dipolar couplings ranged from −0.9 to 0.6 Hz. The small magnitude of the observed dipolar couplings may be explained by motions of the tag which decrease the degree of alignment (Figure 5). To prove that differences in splittings found for zinc- and cobalt-bound proteins are due to dipolar couplings, the field dependence of the splittings was explored at ^{1}H Larmor precession frequencies of 500 and 800 MHz. It is known that the magnitude of dipolar couplings depends on the strength of

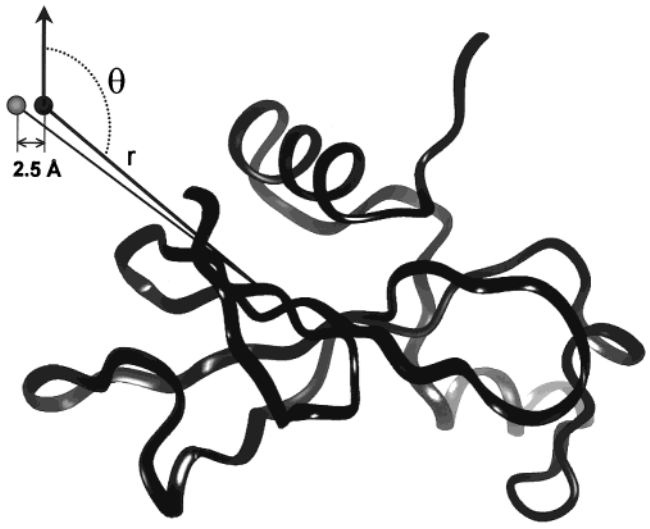

FIGURE 4: Coordinate system defining the parameters *r*, as the distance between the unpaired electron and a nucleus, and θ, as the angle between the electron−nucleus vector and the *z*-axis of the paramagnetic susceptibility tensor. Axial symmetry is assumed. The black circle shows the position of the paramagnetic probe as defined by the Co^{2+}-induced dipolar shifts. The light gray circle demonstrates the position of the paramagnetic center determined by fitting the $Mn^{2+}-H_N$ distances to the crystal structure of barnase (*14*). The distance between the two centers is 2.2 Å.

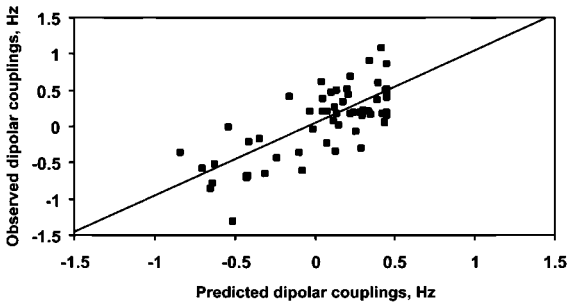

FIGURE 5: Scatter plot showing the correlation between 58 experimentally determined ^{1}H-^{15}N residual dipolar couplings and those obtained based on the crystal structure of barnase (*14*). The predicted values for residual dipolar couplings were obtained using an in-house written tensor fitting routine. The alignment tensor was axial as predicted by EPR. The linear correlation coefficient of 0.72 between the experimental and expected dipolar couplings was observed.

the applied magnetic field. The field dependence of the alignment for the cobalt-bound C-ZFbarnase shows the expected increase in magnitude with increase in external magnetic field.

To demonstrate the crucial role of bound cobalt in the partial alignment of C-ZFbarnase in the magnetic field, 58 dipolar couplings with and without addition of free $CoCl_2$ were measured in barnase(H102A), lacking the metal binding tag. No differences were observed between $^1J_{HN}$ values in barnase(H102A) in the absence and presence of free $CoCl_2$. In addition, $^1J_{HN}$ couplings measured in the zinc-bound protein are not significantly different from those measured in barnase(H102A) in the absence of the tag. This finding indicates that the metal binding tag is not responsible for anisotropic magnetic susceptibility.

The observed H−N dipolar couplings were used in an in-house written alignment tensor fitting program to assess the agreement of the experimental couplings with expected dipolar couplings based on the crystal structure of barnase.

The linear correlation, having an *R* value of 0.72, between experimental and calculated dipolar couplings is shown in Figure 5. The magnitude of the fitted axial component of the magnetic susceptibility was negative as predicted by EPR and determined by dipolar shift tensor fitting procedure. Introduction of rhombicity did not produce a statistically significant improvement of the fit.

DISCUSSION

The presence of a reference frame within paramagnetic proteins provides a unique opportunity to define coordinates of the protein of interest with respect to these axes. However, for nonmetalloproteins there are ways to introduce a unique paramagnetic probe into the protein of interest in order to obtain valuable distance and angular information. Here we utilize a retroviral zinc finger tag fused to the C-terminus of barnase as a site for specific metal attachment. Binding of manganese and cobalt to the zinc finger tag allows introduction of a paramagnetic probe suitable for measurements of unpaired electron$-H_N$ distances, H$-$N residual dipolar couplings, and dipolar shifts in the protein of interest. The mobility of the tag, a possibility of spin delocalization resulting from the relatively large zinc finger cage, inherent uncertainties in $T1$ measurements, and assumptions used to simplify mathematical equations introduce a certain degree of error into the experimental distance measurements. However, average errors of $\pm$4.5 Å do not reduce the structural significance of these long-range distance restraints. The observed dipolar shifts were small in magnitude, which is consistent with the long Mn^{2+} to H_N distances. However, despite these limitations, *z*-projections of the electron$-H_N$ vectors could be obtained with reasonable accuracy, demonstrating the robustness of this approach (Figure 3). The position of the paramagnetic center fitted using distance information deviated by only 2.5 Å from the point independently defined by fitting dipolar shift data to the crystal structure of barnase, demonstrating the self-consistency of the data (Figure 4). The presence of two possible positions of the paramagnetic ion may reflect different averaging of the distances due to r^6 versus r^3 dependence, error contributions to measurements of $Mn^{2+}-H_N$ distances and dipolar shifts, or differences in the binding of Co^{2+} and Mn^{2+}. In addition, the orientation of the paramagnetic susceptibility tensor as defined by distance and angular restraints varied by less than 10° from that determined by fitting residual dipolar couplings to the crystal structure of barnase.

The observed dipolar couplings depend on the strength of the external magnetic field in a predictable manner and are structurally meaningful. The small magnitude of these couplings is consistent with the size of ^1H-^{15}N dipolar couplings observed previously in a paramagnetic system and partly arise from conformational instability at the zinc finger attachment site (Figure 5). Although the use of the a/b TROSY experiment permitted accurate measurement of dipolar couplings under our conditions, when necessary the use of a J-modulated HSQC experiment can provide very accurate measurements of small residual dipolar couplings (*33*).

Research presented in this paper is the first attempt to interpret effects induced by a paramagnetic probe introduced into a nonmetal binding protein in terms of coordinates in the paramagnetic susceptibility axes. The availability of *z*-coordinates should prove valuable in global fold structure determination, in domain orientation within multidomain proteins, and in structure refinement. There are several ways to improve this methodology. For instance, short and more rigid metal-chelating tags can be introduced by chemical modification of protein molecules, permitting the observation of larger dipolar shifts and dipolar couplings. Conjugation of metal-chelating tags also has the advantage of decreasing metal to nuclei distances and allowing a greater range of metal substitutions.

In conclusion, the proposed methodology offers a number of advantages. Rapid affinity purification protocols can be developed based on the metal binding tag. Introduction of metal binding tags at either the N- or the C-terminus of the protein of interest should induce different orientations of the protein molecule in the magnetic field. This will significantly reduce the uncertainty associated with dipolar coupling restraints obtained from a single protein alignment and will allow a more precise determination of H$-$N bond vector positions in the protein structure. Finally, the rapid and straightforward methodology for obtaining unpaired electron$-$nuclear distances and dipolar shifts and for determination of coordinates in the paramagnetic susceptibility tensor will provide a novel and robust approach for fold recognition and additional structural restraints in NMR solution structure determination.

ACKNOWLEDGMENT

We thank Arto Annila and Perttu Permi for providing their a/b TROSY pulse sequence, and Mark Rance for helpful discussions.

REFERENCES

1. Aitio, H., Annila, A., Heikkinen, S., Thulin, E., Drakenberg, T., and Kilpelainen, I. (1999) *Protein Sci. 8*, 2580−2588.
2. Tjandra, N., and Bax, A. (1997) *Science 278*, 1111−1114.
3. Tolman, J. R., Flanagan, J. M., Kennedy, M. A., and Prestegard, J. H. (1995) *Proc. Natl. Acad. Sci. U.S.A. 92*, 9279−9283.
4. Schmiedeskamp, M., and Klevit, R. E. (1997) *Biochemistry 36*, 14003−14011.
5. Ramirez, B. E., and Bax, A. (1998) *J. Am. Chem. Soc. 120*, 9106−9107.
6. Gochin, M. (2000) *Struct. Folding Des. 8*, 441−452.
7. Hus, J. C., Marion, D., and Blackledge, M. (2000) *J. Mol. Biol. 298*, 927−936.
8. Arnesano, F., Banci, L., Bertini, I., Ciofi-Baffoni, S., Woodyear, T. L., Johnson, C. M., and Barker, P. D. (2000) *Biochemistry 39*, 1499−1514.
9. Biekofsky, R. R., Muskett, F. W., Schmidt, J. M., Martin, S. R., Browne, J. P., Bayley, P. M., and Feeney, J. (1999) *FEBS Lett. 460*, 519−526.
10. Banci, L., Bertini, I., Rosato, A., and Scacchieri, S. (2000) *Eur. J. Biochem. 267*, 755−766.
11. Hansen, M. R., Mueller, L., and Pardi, A. (1998) *Nat. Struct. Biol. 5*, 1065−1074.
12. Clore, G. M., and Gronenborn, A. M. (1998) *Curr. Opin. Chem. Biol. 2*, 564−570.
13. Annila, A., Aitio, H., Thulin, E., and Drakenberg, J. (1999) *J. Biomol. NMR 14*, 223−230.
14. Mauguen, Y., Hartley, R. W., Dodson, E. J., Dodson, G. G., Bricogne, G., Chothia, C., and Jack, A. (1982) *Nature 297*, 162−164.
15. Gaponenko, V., Howarth, J. W., Columbus, L., Gasmi-Seabrook, G., Yuan, J., Hubbell, W. L., and Rosevear, P. R. (2000) *Protein Sci. 9*, 302−309.

16. Bycroft, M., Ludvigsen, S., Fersht, A. R., and Poulsen, F. M. (1991) *Biochemistry 30*, 8697−8701.
17. Hartley, R. W. (1993) *Biochemistry 32*, 5978−5984.
18. Hartley, R. W., and Rogerson, D. L., Jr. (1972) *Prep. Biochem. 2*, 229−242.
19. Xu, B., Trawick, B., Krudy, G. A., Phillips, R. M., Zhou, L., and Rosevear, P. R. (1994) *Biochemistry 33*, 398−402.
20. Werst, M. M., Davoust, C. E., and Hoffman, B. M. (1991) *J. Am. Chem. Soc. 113*, 1533−1538.
21. Ferretti, J. A., and Weiss, G. H. (1989) *Methods Enzymol. 176*, 3−11.
22. Weber, D. J., Mullen, G. P., and Mildvan, A. S. (1991) *Biochemistry 30*, 7425−7437.
23. Mildvan, A. S., Granot, J., Smith, G. M., and Liebman, M. N. (1980) Nuclear Magnetic Relaxation Rates. In *Methods for Determining Metal Ion Environments in Proteins*, Vol. 2, pp 211−235, Elsevier North-Holland, Inc., Amsterdam, The Netherlands.
24. Solomon. (1955) *Phys. Rev. 99*, 559−565.
25. Green, L. M., and Berg, J. M. (1989) *Proc. Natl. Acad. Sci. U.S.A. 86*, 4047−4051.
26. Thiesen, H. J., and Bach, C. (1991) *Biochem. Biophys. Res. Commun. 176*, 551−557.
27. Mazumder, A., Neamati, N., Ojwang, J. O., Sunder, S., Rando, R. F., and Pommier, Y. (1996) *Biochemistry 35*, 13762−13771.
28. Jones, D. N., Bycroft, M., Lubienski, M. J., and Fersht, A. R. (1993) *FEBS Lett. 331*, 165−172.
29. Berry, M. B., and Phillips, G. N., Jr. (1998) *Proteins: Struct., Funct., Genet. 32*, 276−288.
30. Loria, J. P., and Nowak, T. (1998) *Biochemistry 37*, 6967−6974.
31. Hoffman, B. M., Weschler, C. J., and Basolo, B. (1976) *J. Am. Chem. Soc. 98*, 5473−5482.
32. Andersson, P., Annila, A., and Otting, G. (1998) *J. Magn. Reson. 133*, 364−367.
33. Tolman, J. R., and Prestegard, J. H. (1996) *J. Magn. Reson. B 112*, 245−252.

BI001381W